RESEARCH ARTICLE

Diallyl disulfide inhibits growth and metastatic potential of human triple-negative breast cancer cells through inactivation of the β-catenin signaling pathway

*Jing Huang[1], Bing Yang[1], Tingxiu Xiang[1], Weiyan Peng[1], Zhu Qiu[1], Jingyuan Wan[2], Li Zhang[3], Hongyuan Li[1], Hongzhong Li[1] and Guosheng Ren[1]**

[1] Molecular Oncology and Epigenetics Laboratory, The First Affiliated Hospital of Chongqing Medical University, Chongqing, P. R. China
[2] Department of Pharmacology, Chongqing Medical University, Chongqing, P. R. China
[3] Department of Pathophysiology, Chongqing Medical University, Chongqing, P. R. China

Received: September 24, 2014
Revised: January 15, 2015
Accepted: February 20, 2015

Scope: Although diallyl disulfide (DADS), an important garlic (*Allium sativum*) derivative, has exhibited potential anticancer activity, the molecular mechanism of this activity remains unknown. In this study, we evaluated the antitumor activity of DADS in triple-negative breast cancer (TNBC) cell lines based in vitro and in vivo models.

Methods and results: We found that treatment with DADS resulted in decreased viability, increased apoptosis, and suppression of metastatic potential in TNBC cells. Furthermore, DADS induced dysregulation of B-cell lymphoma (Bcl)-2 family members, downregulation of matrix metalloproteinase (MMP)-9 and reversal of the epithelial–mesenchymal transition (EMT). Interestingly, DADS significantly inhibited activation of the β-catenin signaling pathway, which regulated Bcl-2 family members, MMP-9 and EMT in TNBC cells. Consistent with these in vitro findings, we also verified the anticancer potential of DADS in MDA-MB-231 xenograft mice. Treatment with DADS significantly reduced tumor volume and weight and increased apoptosis in these mice, while the expression of active β-catenin was decreased, and the downstream molecules were dysregulated.

Conclusion: Our results show that the antitumor effect of DADS on TNBC cells is mediated by the β-catenin pathway, suggesting that DADS could be used as a potential therapeutic agent for treating or preventing breast cancer.

Keywords:
β-catenin / Diallyl disulfide / Epithelial–mesenchymal transition / Matrix metalloproteinase / Triple-negative breast cancer

1 Introduction

Breast cancer is the most commonly diagnosed cancer and the leading cause of cancer death worldwide in females. Triple-negative breast cancers (TNBCs), which do not express the genes for estrogen receptor, progesterone receptor, and human epidermal growth factor receptor-2, account for approximately 15% of all breast cancers. Patients with TNBC generally have an increased risk of cancer progression and exhibit poorer overall survival. Furthermore, TNBC does not respond to endocrine therapy or other available targeted agents other than traditional cytotoxic chemotherapy which is frequently trapped in drug resistance [1–3]. Therefore, the identification of new drugs or treatments for TNBC is imperative.

Because an increasing number of natural herbal substances have been shown to inhibit breast cancer development and progression, botanical medicines have attracted

Correspondence: Dr. Hongzhong Li, Molecular Oncology and Epigenetics Laboratory, The First Affiliated Hospital of Chongqing Medical University, No.1 Youyi Road, Yuzhong District, Chongqing, 400016, P. R. China
E-mail: tibetlhz@126.com
Fax: +86-2389012305

Abbreviations: **Bcl**, B-cell lymphoma; **DADS**, diallyl disulfide; **EMT**, epithelial–mesenchymal transition; **MMP**, matrix metalloproteinase; **TIMP**, tissue inhibitors of metalloproteinase; **TNBC**, triple-negative breast cancer

*Additional corresponding author: Professor Guosheng Ren, E-mail: rengs726@126.com
Colour Online: See the article online to view Fig. 1, 5, 8 in colour.

recent attention in the search for effective anticancer drugs. Botanical medicines are also considered a practical approach for reducing the ever-increasing incidence of breast cancer, as they can be administered as dietary supplements [4, 5]. Diallyl disulfide (DADS), an oil-soluble compound extracted from garlic, demonstrates a variety of pharmacological and biological activities, including anti-inflammatory, antimicrobial, and antitumor activities [6–8]. Although a growing body of evidence indicates that DADS inhibits gastric, hepatic, prostate, and lung cancer progression by inducing apoptosis and inhibiting cell cycle arrest and metastasis, the molecular mechanism by which DADS inhibits TNBC cell growth and metastatic potential remains unclear [9–12]. In this study, we used in vitro and in vivo TNBC models to investigate the anticancer activity of DADS. We show that DADS induces apoptosis, suppresses metastatic potential, and reverses the epithelial–mesenchymal transition (EMT) by downregulating the β-catenin pathway. These findings suggest that DADS is a very promising candidate for breast cancer intervention and prevention.

2 Materials and methods

2.1 Reagents and cell lines

DADS ($C_6H_{10}S_2$, MW: 146.28, shown in Fig. 1A) was purchased from Cayman Chemical Co. (Ann Arbor, MI, USA), and the purity was determined by HPLC, as previously described [13]. The human TNBC cell lines MDA-MB-231, MDA-MB-468, and BT-549 were obtained from American Type Culture Collection (ATCC, Rockville, MD, USA) and cultured in RPMI-1640 supplemented with 10% FBS and 1% penicillin/streptomycin. The cells were incubated at 37°C in a humidified atmosphere containing 5% CO_2.

2.2 Cell viability assay

The cells were seeded into 96-well plates (4000 cells/well), treated with 100 μl medium plus dimethyl sulfoxide (DMSO) (vehicle control, final concentration: <0.5% DMSO) or DADS (final concentration: 50, 100, 200, or 400 μM) and incubated for 48 h. The cell viability was then measured using a CCK-8 kit (KeyGEN Biotech, Nanjing, China). Each plate included a control well that contained medium without cells, which was used to obtain a background spectrometric absorbance value that was subtracted from the test sample readings. The data are expressed as the mean ratio of live cells (treated versus control) ± SD for three replicates.

2.3 Flow cytometric analysis of cell apoptosis

For the apoptosis analysis, we performed Annexin V-FITC/propidium iodide staining (KeyGEN Biotech) according to the manufacturer's instructions and analyzed the cells on an Elite ESP flow cytometer.

2.4 Caspase activity assay

Caspase 3 and caspase 9 activities were measured using colorimetric assay kits (Beyotime Institute of Biotechnology, Jiangsu, China) according to the manufacturer's instructions. Briefly, after isolation by two-step collagenase digestion, the breast cancer cells were mixed with 50 μl cold lysis buffer. The supernatant (10 μl) was then mixed with 10 μl caspase substrate and 80 μl reaction buffer and incubated at 37°C for 2 h in the dark. The fluorescence intensity of the caspase substrate at 405 nm was measured using a microplate reader. The caspase activity was calculated as the OD_{405} per 100 μg protein.

2.5 Western blotting

The cell lysate was prepared using a protein extraction kit (Active Motif Company, Carlsbad, CA USA) according to the manufacturer's instructions. The protein concentrations were determined using a BCA protein assay kit (Pierce Biotechnology, Inc., Rockford, IL, USA). The cell lysate was subjected to western blot analysis using antibodies to B-cell lymphoma (Bcl-2), Bcl-xl, Bax, Bad, Bak, MMP-9, E-cadherin, Vimentin, N-cadherin, Snail, total β-catenin, active β-catenin, and β-actin (Cell Signaling Technology, Inc., Danvers, MA, USA and Abcam, Inc., Cambridge, MA, USA). Antibody binding was visualized by ECL chemiluminescence system and brief exposure of the membranes to X-ray films (Kodak Company, Tokyo, Japan).

2.6 Wound healing assay

The cancer cells were cultured in 6-well plates in medium containing 10% FBS. When the cells were nearly confluent, the cell monolayer in each well was carefully scratched with a plastic pipette tip to create a linear "wound". The monolayer was washed twice with PBS to remove debris and detached cells, and the cells were then exposed to serum-free medium with or without different concentrations of DADS (12.5, 25, or 50 μM) for 12 h. The wound closure was monitored and photographed using a microscope fitted with a Leica camera. By comparing the images from when the wound was generated to the last time point (12 h), the degree of wound closure was then quantitatively evaluated using Image-Pro Plus software. Four fields from each well were documented, and each experiment was performed in triplicate.

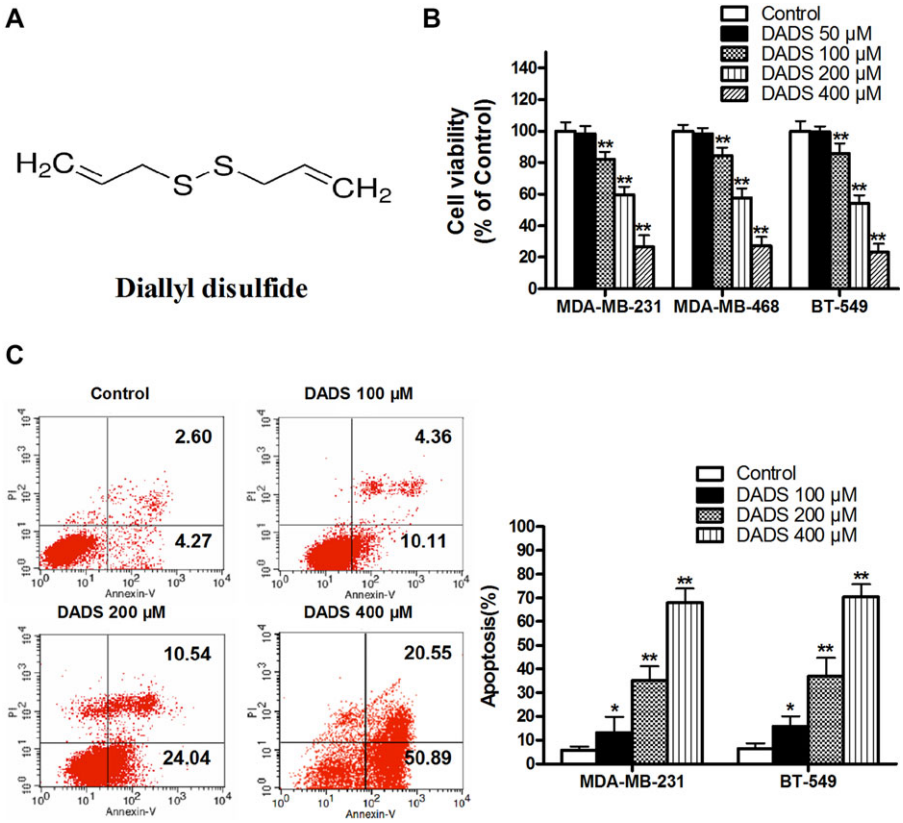

Figure 1. DADS inhibits cell proliferation and induces apoptosis in TNBC cells. (A) Chemical structure of DADS. (B) Breast cancer cell lines were treated with various concentrations of DADS for 48 h, and cell viability was measured using a CCK-8 kit. The data are expressed as the ratio of treated cells to control cells. (C) DADS-induced apoptosis was examined in MDA-MB-231 and BT-549 cells by flow cytometric analysis of Annexin V-FITC/propidium iodide staining. The numbers inside the dot plots indicate the percentage of apoptotic MDA-MB-231 cells. All experiments were performed thrice in triplicate. The data are expressed as the mean ± SD. $*p < 0.05$ and $**p < 0.01$ (versus control group).

2.7 Cell migration and invasion assays

The cancer cell migration/invasion assays were conducted with transwell membranes (8 μm pore size, 24-well plate, BD Biosciences, Billerica, MA, USA). For the migration assay, normal or adenovirus-transfected cancer cells were trypsinized, washed, and suspended in medium without FBS. Migration-inducing medium (with 10% FBS) was added to the lower wells. Cells suspended in serum-free medium containing various concentrations of DADS (12.5, 25, or 50 μM) were added to the upper wells (20 000 cells/well). After 24 h, the top surface of the chambers was scraped clean with a cotton swab. The cells on the lower surface of the membranes were fixed for 15 min with methanol and then stained with Giemsa solution. Completed transmigration was evaluated by microscopy. Four random fields per filter were scanned for the presence of cells on the lower side of the membrane. For the cell invasion assay, the transwell membranes were first coated with 100 μl Matrigel matrix (1 mg/ml, BD Biosciences). The experiment was then carried out as for the migration assay.

2.8 Human MMP antibody array

The expression profile of MMP-related proteins was analyzed using a human MMP array kit (AAH-MMP-1, RayBiotech, Inc., Norcross, GA, USA), which contains duplicate spots of 10 MMP-related proteins (Fig. 4A). Briefly, each captured antibody was printed on the membrane, and then treated or untreated cell lysate was added to the antibody array membranes. After extensive washing, the membranes were incubated with a cocktail of biotin-conjugated antiapoptotic protein antibodies. After incubation with HRP-streptavidin, the signals were visualized by chemiluminescence. The relative expression levels of target proteins were determined by comparing the signal intensities quantified by densitometry. A positive control was used to normalize the results from the different membranes.

2.9 Active human MMP-9 fluorescence assay

MMP-9 activity was quantified using ELISA-based activity assays (F9M00, R&D systems, Inc., Minneapolis, MN, USA) according to the manufacturer's instructions. Briefly, the breast cancer cells were treated with different concentrations of DADS for 48 h. The cell culture supernatants from treated or untreated cells were then collected and assayed for MMP-9 activity. The samples and standards were incubated for 2 h at room temperature in 96-well plates coated with monoclonal antibodies for MMP-9, then chemically activated with p-aminophenylmercuric acetate. After incubation for another 2 h at 37°C, a fluorogenic substrate was added to each well, and

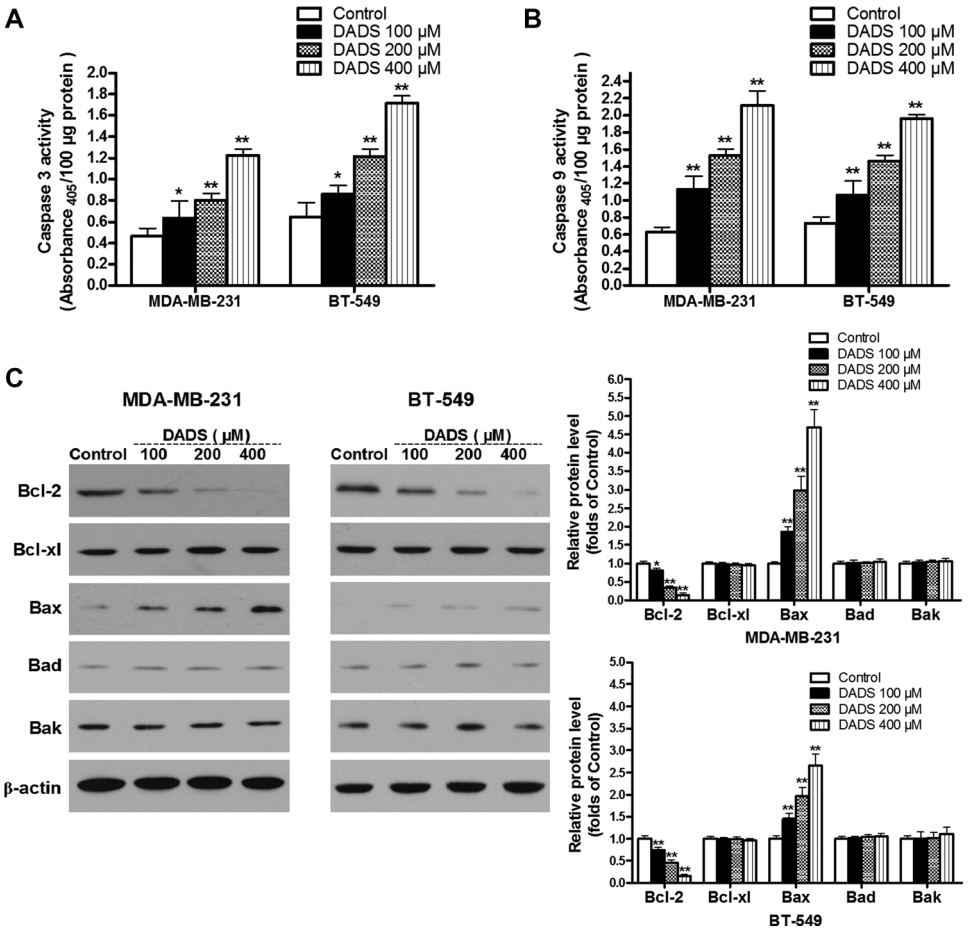

Figure 2. DADS induces caspase activation and regulates the expression of Bcl-2 family proteins in TNBC cells. (A, B) Caspase 3 and caspase 9 activities were measured using colorimetric assay kits. The data are expressed as the absorbance at 405 nm per 100 μg protein. (C) The effect of DADS treatment on the expression of Bcl-2 family members was measured by Western blotting. β-actin was used as a loading control. The data are presented as the mean ± SD ($n \geq 6$). *$p < 0.05$ and **$p < 0.01$ (versus control group).

the plate was incubated at 37°C for 20 h in dark humidified environment. The plate was then read on a spectrophotometer with excitation and emission wavelengths of 320 and 405, respectively. The data were quantified using standard curves generated from reagents provided with the kit.

2.10 Indirect immunofluorescence analysis

For the immunofluorescence experiments, the cells were prepared and analyzed under a fluorescence microscope (Leica DM IRB) as described previously [14]. Briefly, the cells were incubated with a primary antibody to E-cadherin or Vimentin (Cell Signaling Technology, Inc.) and then with the DyLight 549 or DyLight 488 antirabbit IgG secondary antibody (CW-Biotech, Beijing, China). The cells were then counterstained with DAPI and imaged with a fluorescence microscope.

2.11 Adenovirus infection

For this study, we used adenovirus expressing empty Ad-Easy1 vector, β-catenin, scrambled siRNA or β-catenin siRNA, as described previously [15, 16]. In addition to expressing transgenes, the adenovirus expression system also includes RFP as a marker for monitoring transfection efficiency. We conducted a series of infections with various dilutions of adenovirus to determine the optimal multiplicity of infection for expressing the target genes and minimizing cytotoxicity. After 48 h of transfection, the efficiency of β-catenin expression was assessed by real-time PCR and Western blotting.

2.12 Quantitative real-time polymerase chain reaction

Real-time PCR was carried out using an ABI 7500 Real-Time PCR System (Applied Biosystems) and the Maxima SYBR Green/ROX qPCR Master Mix (MBI Fermentas, St. Leon-Rot, Germany). The primer pairs were as follows: (i) β-catenin, 5′-TGTATGAGTGGGAACAGGGATT-3′ (forward) and 5′-GCCAAACGCTGGA CATTAGT-3′ (reverse); and (ii) β-actin, 5′-CCTGTGGCATCCACGAAACT-3′ (forward) and 5′-GAAGCATTTGCGGTGGACGAT-3′ (reverse). These primer pairs amplified 170 and 314 bp products, respectively. The thermal cycling conditions were as follows: 95°C for 30 s, 5 s at 95°C, 1 min at 60°C for 40 cycles. We

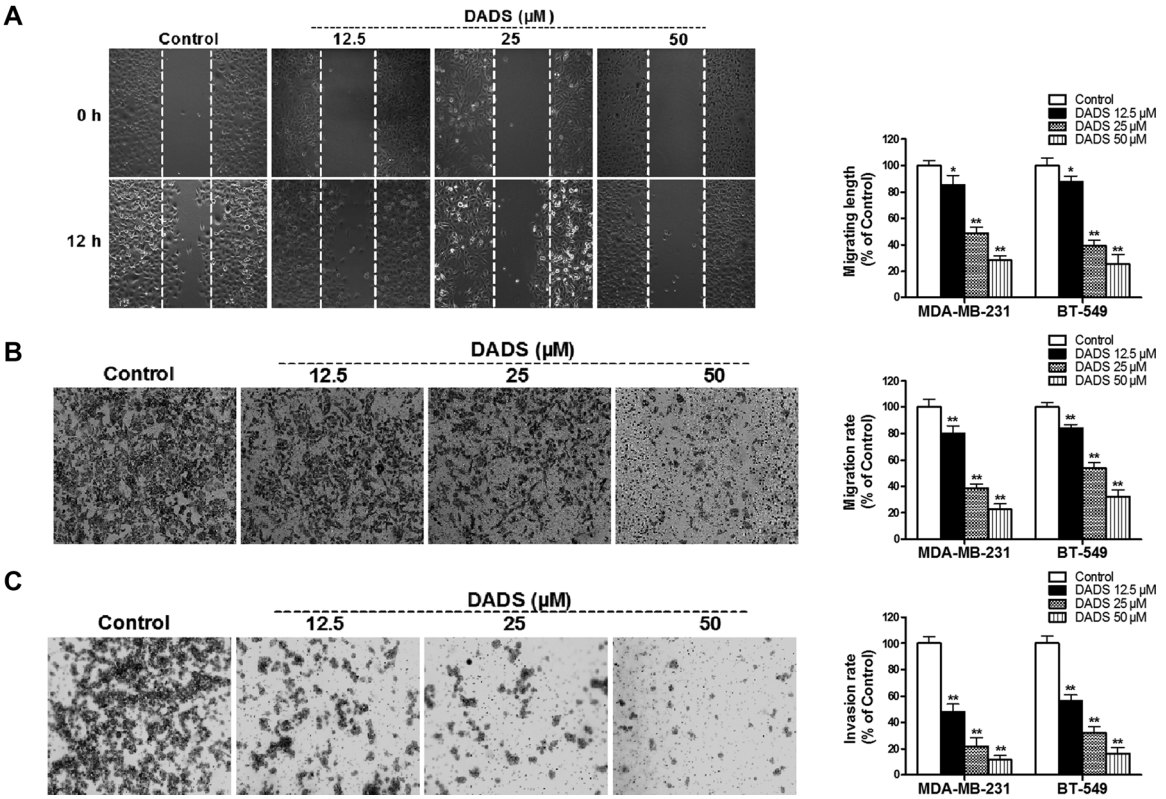

Figure 3. DADS inhibits TNBC cell migration and invasion. (A) For the wound healing assay, confluent monolayers of MDA-MB-231 and BT-549 cells were scarred, and the cells were treated for 12 h with different concentrations (12.5, 25, or 50 μM) of DADS or the vehicle only (DMSO). The migration of the cells into the wound zone was monitored by microscopy over a 12-h period. The panel on the left shows the wound healing assay in MDA-MB-231 cells. Black lines indicate the scraped zone. Summary of results from the transwell migration assay (B) and the Matrigel invasion assay (C). After 24 h of incubation with or without DADS, the cells that migrated to the lower chamber or invaded through the Matrigel were fixed, stained, and counted using a light microscope. Four random fields per filter were scanned for the presence of cells on the lower side of the membrane. The panels on the left figures show the cell migration assay and the invasion assay, respectively, in MDA-MB-231 cells. All experiments were performed thrice in triplicate. The data are presented as the mean ± SD. $*p < 0.05$ and $**p < 0.01$ (versus control group).

further performed a melting-curve analysis and agarose gel electrophoresis of the PCR products. The relative expression levels of β-catenin in cancer cells were standardized to β-actin expression levels.

2.13 Animal experiments

All of the animal studies were approved by the Animal Ethics Committee of Chongqing Medical University (Approval number: SCXK2012-0001). Five-week-old severe combined immunodeficiency hairless female mice were purchased from the Institute of Laboratory Animal Science (Chinese Academy of Medical Science, Beijing, China) and randomly divided into two groups of nine mice each. The mice were housed according to national and institutional guidelines for humane animal care. The mice were injected subcutaneously with MDA-MB-231 cells (2×10^6) on the right rear flank, and were then injected intraperitoneally (i.p.) once every 4 days with 100 μl of vehicle only (PBS) or DADS (100 mg/kg weight) [9,17]. The general health of the mice was closely monitored every other day. Food consumption and body weight were used as general health indicators throughout the experiments. The tumor diameters were measured every week, and the tumor volumes were calculated according to the following formula: tumor volume (mm^3) = 0.5 × length (mm) × width^2 (square mm). After 4 weeks of treatment, the mice were euthanized via CO_2 asphyxiation. The tumors were then removed, weighed, and sent for immunohistochemistry (IHC) analysis.

2.14 Immunohistochemistry

The tumor tissues were fixed in 4% formaldehyde solution (pH 7.0) and then embedded in paraffin. The immunohistochemical studies were performed using the UltraSensitive TM SP Kit (Maixin-Bio, Fujian, China) according to the manufacturer's instructions. The tumor specimens were stained

A

POS	POS	NEG	NEG	MMP-1	MMP-2	MMP-3	MMP-8
POS	POS	NEG	NEG	MMP-1	MMP-2	MMP-3	MMP-8
MMP-9	MMP-10	MMP-13	TIMP-1	TIMP-2	TIMP-4	NEG	POS
MMP-9	MMP-10	MMP-13	TIMP-1	TIMP-2	TIMP-4	NEG	POS

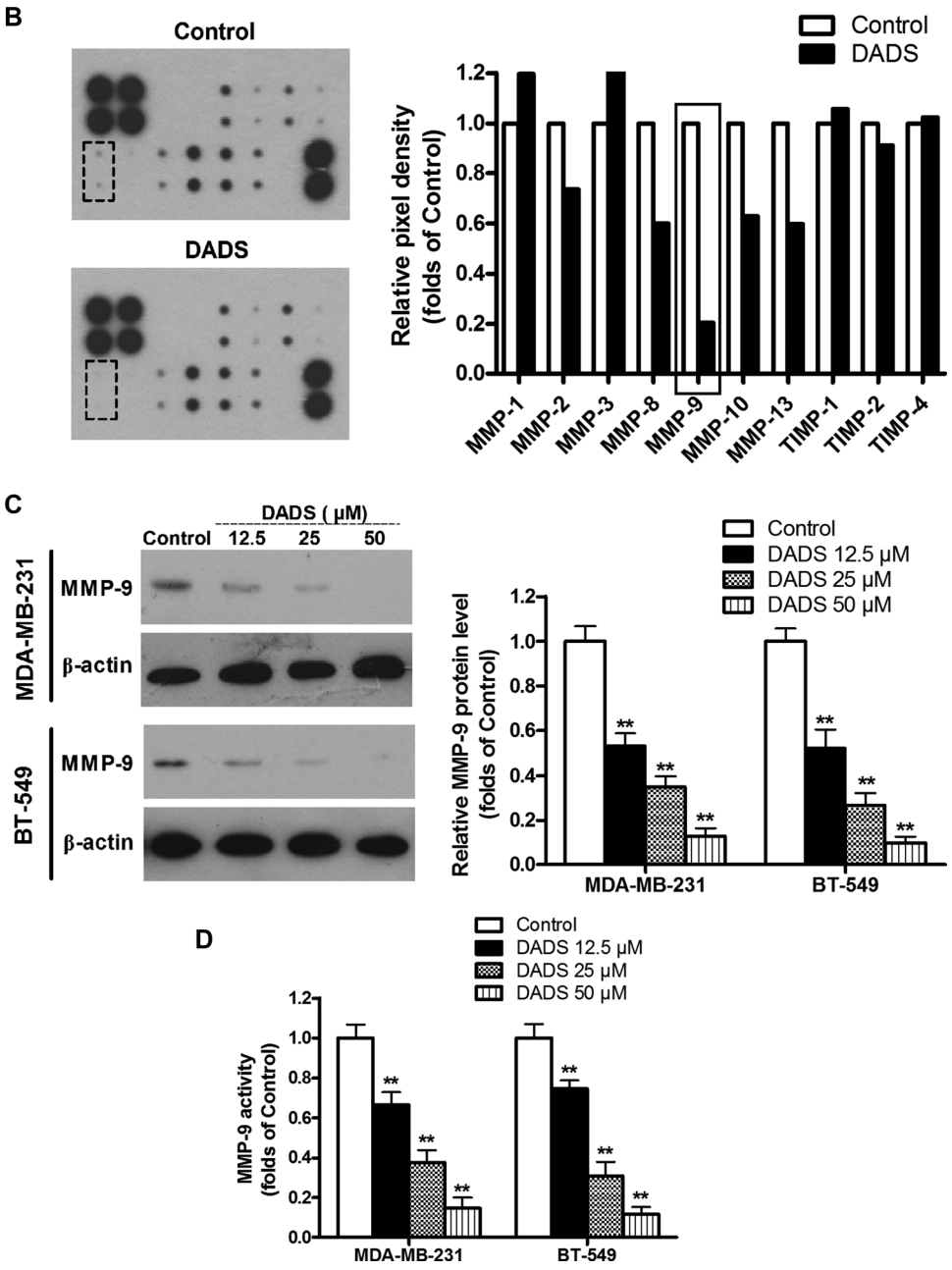

Figure 4. Downregulation of MMP-9 in TNBC cells treated with DADS. (A) Template showing the location of the MMP/TIMP antibodies spotted onto the RayBio Human MMP Array Kit. POS: positive; NEG: negative. (B) DADS-induced modulation of MMP/TIMP proteins in MDA-MB-231 cells. MDA-MB-231 cells were treated with DADS (25 μM) for 48 h, and the cell lysate was applied to the antibody array. The pixel density was measured, and the data are presented as ratios (compared to the control). Proteins exhibiting a ratio ≥2 are indicated with black boxes. (C) MMP-9 expression in MDA-MB-231 and BT-549 cells was assessed by Western blot. β-actin was used as an internal loading control. The blots shown are representative of six independent experiments. The data are presented as the mean ± SD. $^{**}p < 0.01$ (versus control group). (D) MMP-9 activity in supernatant collected from untreated or DADS-treated cells was detected using an active human MMP-9 fluorescence assay. The experiments were performed thrice in triplicate. The data are presented as the mean ± SD. $^{**}p < 0.01$ (versus control group).

with a cleaved caspase 3 antibody (Cell Signaling Technology, Inc.) to assess apoptosis. A negative control was performed by replacing the primary antibody with PBS. A blinded evaluation of the immunostained slides was performed by a trained pathologist using a light microscope.

2.15 Statistical analysis

The data are presented as the mean ± standard deviation (SD). All statistical analysis was performed using the Student's *t*-test or one-way ANOVA followed by Tukey post hoc

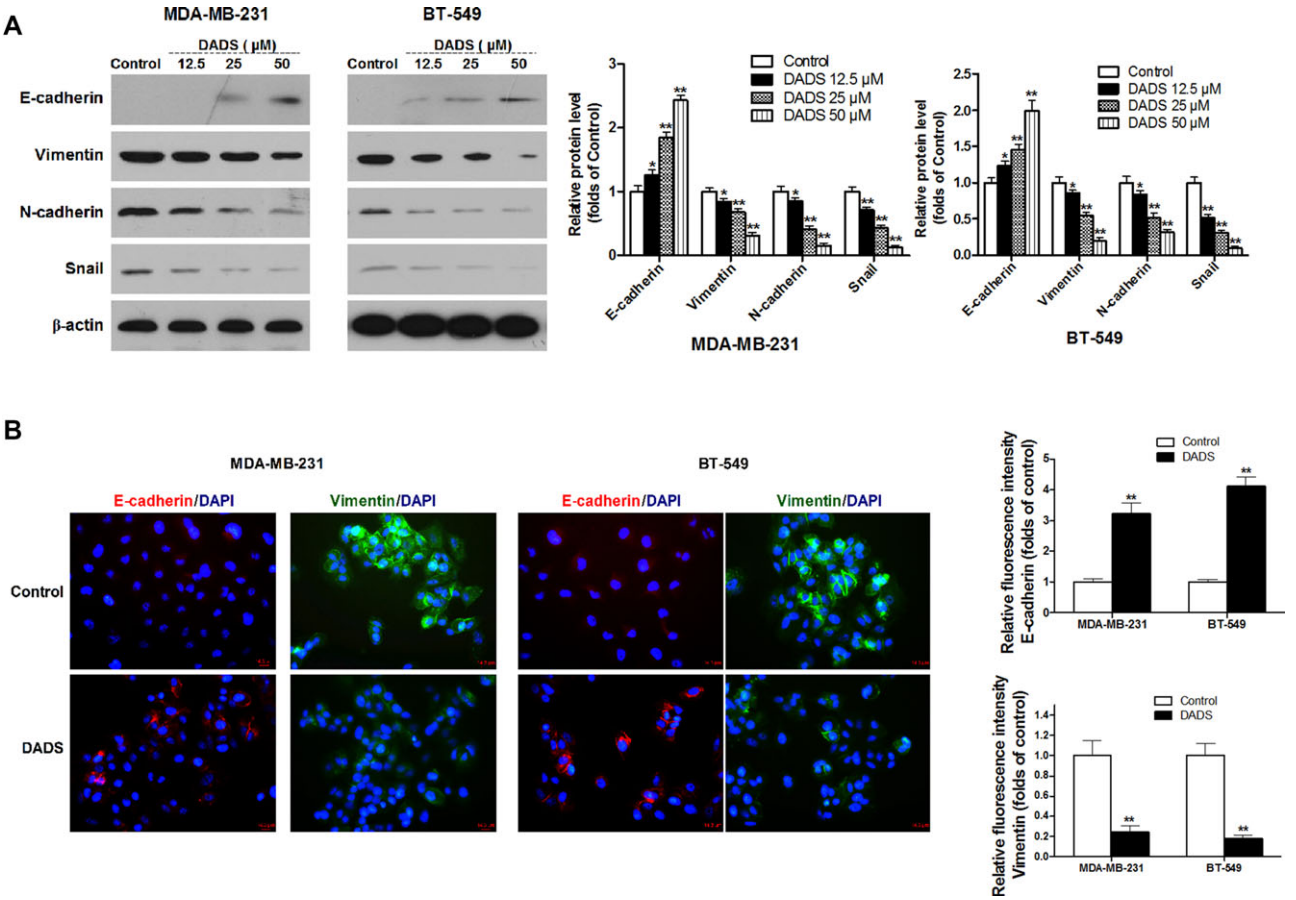

Figure 5. Treatment with DADS reverses EMT in TNBC cells. (A) The effect of DADS treatment on the expression of EMT markers was detected by Western blot. β-actin was used as an internal loading control. The blots shown are representative of six independent experiments. The data are presented as the mean ± SD. $*p < 0.05$ and $**p < 0.01$ (versus control group). (B) Immunostaining showed the upregulation of E-cadherin and downregulation of Vimentin in cells treated with DADS (50 μM) (original magnification: 400×). The nucleus is stained with DAPI (blue), E-cadherin is stained with DyLight 549 (red), and Vimentin is stained with DyLight 488 (green). The experiments were performed thrice in triplicate. The data are presented as the mean ± SD. $**p < 0.01$ (versus control group).

test with Prism GraphPad 4 software (GraphPad Software, Inc.). Differences were considered significant when the *p* values were < 0.05.

3 Results

3.1 DADS inhibits cell proliferation and induces apoptosis in TNBC cells

In our preliminary study, we found that IC50 (48 h) of DADS for MDA-MB-231 cells and BT-549 cells was 282 and 276 μM, respectively (data not shown). Based on this and related studies, we first evaluated the effect of DADS on cell proliferation at concentrations (50, 100, 200, or 400 μM) [9–11]. As shown in Fig. 1B, we observed that DADS inhibited the proliferation of MDA-MB-231, MDA-MB-468, and BT-549 breast cancer cells in a dose-dependent manner. To determine whether the decreased cell proliferation was due to cell death, we detected cell apoptosis by flow cytometry. Following treatment with DADS (100, 200, or 400 μM) for 48 h, we detected significant increased apoptosis in MDA-MB-231 and BT-549 cells, which might contribute to the decreased cell viability (Fig. 1C).

3.2 DADS induces caspase activation and regulates the expression of Bcl-2 family proteins in TNBC cells

Caspases and Bcl-2 family members are crucial mediators of apoptosis [18, 19]. To determine whether DADS promotes apoptosis, we analyzed the activity of key caspases such as caspase 3 and caspase 9 and the expression of important Bcl-2 family members including Bcl-2, Bcl-xl, Bax, Bad, and Bak in MDA-MB-231 and BT-549 cancer cells. As shown in Fig. 2A and B, there was a marked increase in caspase 3 and caspase 9 activities in DADS-treated cancer cells compared to the control cells. In addition, the antiapoptotic factor

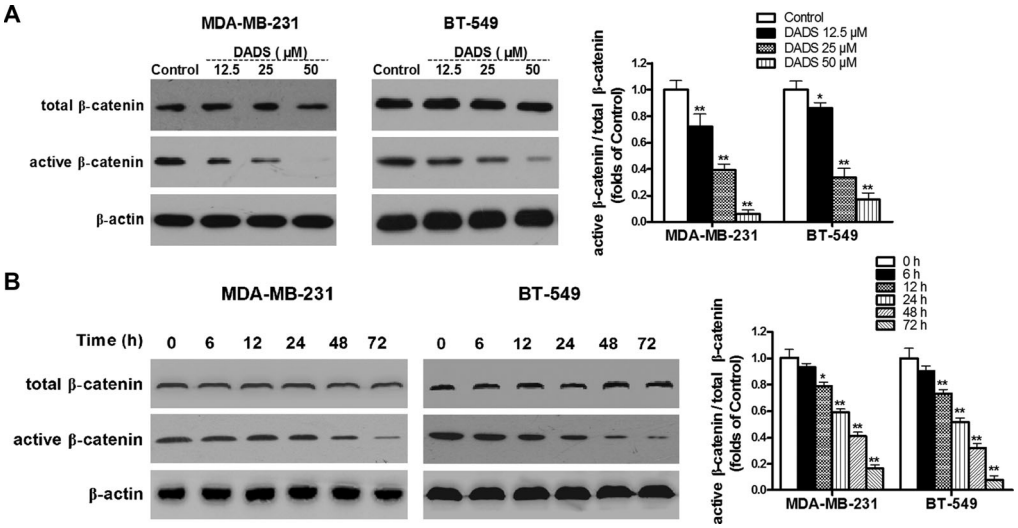

Figure 6. Treatment with DADS suppressed activation of the β-catenin signaling pathway in TNBC cells. (A) Breast cancer cells were treated with various concentrations of DADS for 48 h, and the expression of total or active β-catenin was then measured by Western blot. (B) Breast cancer cells were treated with DADS (25 μM) for different time periods, and the expression of total or active β-catenin was then measured by Western blot. In these assays above, β-actin was used as an internal loading control. The blots shown are representative of six independent experiments. The data are presented as the mean ± SD. $*p < 0.05$ and $**p < 0.01$ (versus control group).

Bcl-2 was downregulated, while the proapoptotic factor Bax was upregulated in response to DADS treatment in TNBC cells (Fig. 2C).

3.3 DADS inhibits TNBC cell migration and invasion

TNBC is associated with an increased risk of visceral metastasis [20]. Therefore, inhibiting the powerful metastatic activity of TNBC cells is essential for improving the prognosis of TNBC patients. Because DADS inhibited cell proliferation at concentrations greater than 50 μM, we next tested the effect of DADS on human breast cancer metastasis at concentrations below 50 μM, as determined by wound healing, transwell migration, and invasion assays. As shown in Fig. 3A and B, in both the wound healing and transwell migration assays, DADS effectively inhibited cancer cell migration in a dose-dependent manner. Moreover, treating MDA-MB-231 or BT-549 cells with increasing doses of DADS significantly reduced the number of cells that invaded the Matrigel-coated wells (Fig. 3C).

3.4 Downregulation of MMP-9 in TNBC cells treated with DADS

Matrix metalloproteinases (MMPs) and tissue inhibitors of metalloproteinases (TIMPs), which function in remodeling the extracellular matrix (ECM), play a significant role in tumor invasion and metastasis [21]. To identify MMPs that are involved in DADS-mediated inhibition of cancer cell migration and invasion, we performed a human MMP array using MDA-MB-231 cells. As shown in Fig. 4B and D, MMP-9 was downregulated by DADS treatment. We confirmed this by Western blotting and MMP-9 activity assays. Similarly, decreased MMP-9 expression and activity were observed in DADS-treated BT-549 cells. These results strongly suggest that downregulation of MMP-9 could be involved in the antimetastatic activity of DADS.

3.5 DADS reverses EMT in TNBC cells

The most comprehensive theory describing how initially quiescent tumor cells acquire metastatic capability is the EMT [22]. We next evaluated the effect of DADS on EMT in the MDA-MB-231 and BT-549 cell lines. As shown in Fig. 5A, DADS-treated cancer cells exhibited increased expression of the epithelial marker E-cadherin and decreased expression of mesenchymal markers such as Vimentin, N-cadherin, and Snail, as determined by Western blotting. Consistent with these results, we also detected increased expression of E-cadherin and decreased expression of Vimentin by immunofluorescence (Fig. 5B). Taken together, these observations suggest that DADS induces a switch from the mesenchymal to the epithelial phenotype in breast cancer cells.

3.6 DADS inhibits cancer cell growth and metastatic potential through inactivation of the β-catenin pathway

Aberrant activation of the β-catenin signaling pathway is frequently involved in breast cancer development and

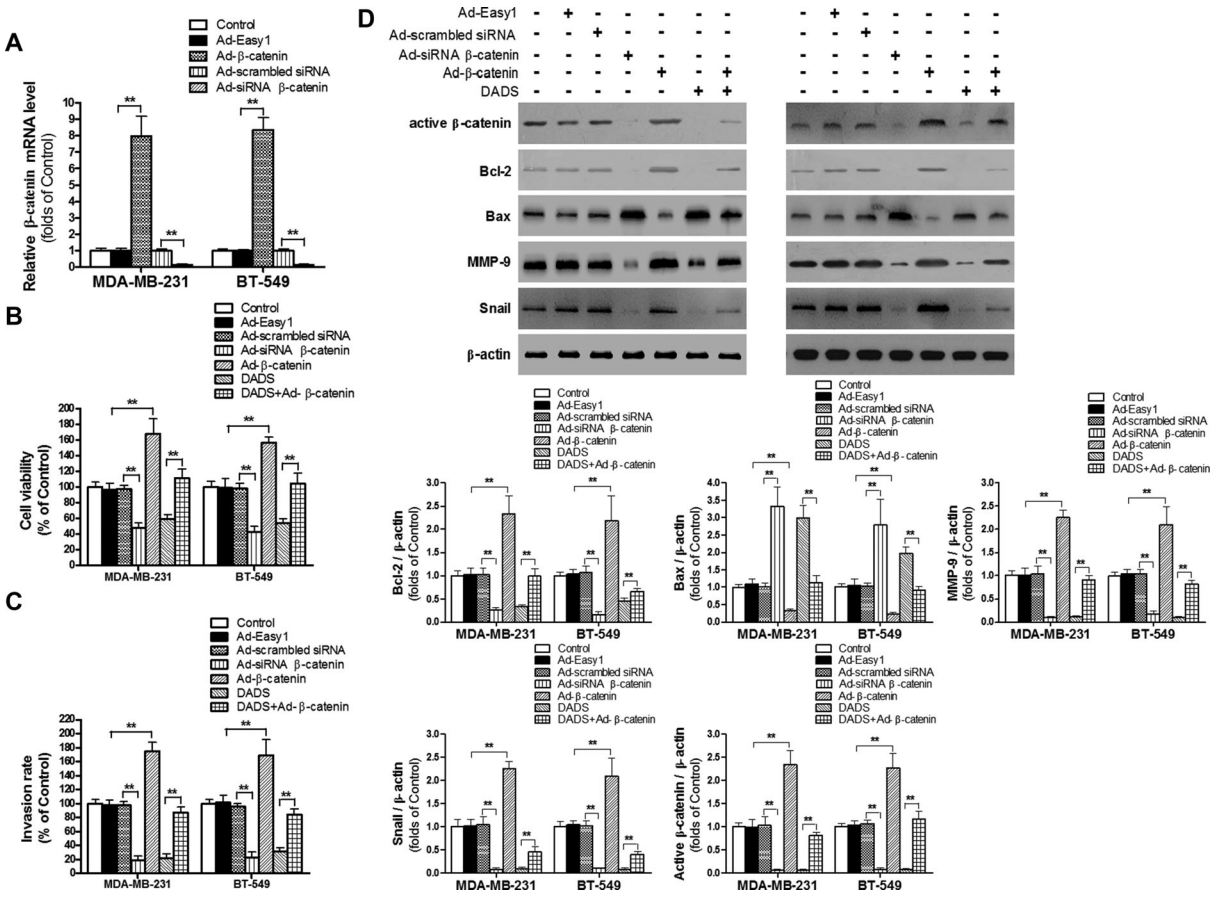

Figure 7. Inactivation of the β-catenin signaling pathway is responsible for the antitumor activity of DADS in TNBC cells. (A) The level of β-catenin mRNA expression in cancer cells transfected with Ad-Easy1, Ad-scrambled siRNA, Ad-si β-catenin, or Ad-β-catenin was determined by real-time PCR. (B) Cell viability assay. Breast cancer cells transfected with Ad-Easy1, Ad-scrambled siRNA, Ad-si β-catenin, or Ad-β-catenin were treated with DADS (200 μM) or left untreated for 48 h, and the cell viability was measured using a CCK-8 kit. The data are expressed as ratios of live treated cells to live control cells. (C) The effect of β-catenin on the metastatic potential of breast cancer cells treated with DADS (25 μM) or left untreated was measured by a cell invasion assay. The experiments described above were performed thrice in triplicate. The data are presented as the mean ± SD. $^{**}p < 0.01$. (D) Cells transfected with Ad-Easy1, Ad-scrambled siRNA, Ad-si β-catenin, or Ad-β-catenin were treated with DADS (200 μM) or left untreated for 48 h, and the expression of related proteins was then measured by Western blot. β-actin was used as an internal loading control. The blots shown are representative of six independent experiments. The data are presented as the mean ± SD. $^{**}p < 0.01$.

progression, due to the modulation of multiple related molecules [23]. We therefore determined whether treatment with DADS affected activation of this pathway. Western blot analysis revealed that activation of the β-catenin pathway in both MDA-MB-231 and BT-549 cells was downregulated by DADS at a dose- and time-dependent manner (Fig. 6). Moreover, overexpression of β-catenin using an adenovirus expression system increased TNBC cell malignancy and reversed the anticancer activity of DADS. In contrast, abrogating β-catenin through the expression of a β-catenin siRNA led to a decrease in cell viability and suppression of metastatic potential in TNBC cells (Fig. 7A–C). More importantly, we observed that regulation of the β-catenin signaling pathway resulted in the modulation of Bcl-2, Bax, MMP-9, and Snail expression in TNBC cells, which strongly suggests that inhibition of the β-catenin signaling pathway is closely involved in DADS-induced antitumor activity in breast cancer cells (Fig. 7D).

3.7 In vivo antitumor activity of DADS

MDA-MB-231 xenograft model was used to evaluate the antitumor potential of DADS in vivo. As shown in Fig. 8A and B, mice treated with DADS exhibited smaller tumor volumes and lower tumor weights compared to the control mice. Intraperitoneal administration of DADS had no detectable toxicity, as there were no differences in body weight between the control and treatment groups, and no signs of adverse health reactions, pain, or distress were observed. Consistent with the in vitro experiments, we detected a significant

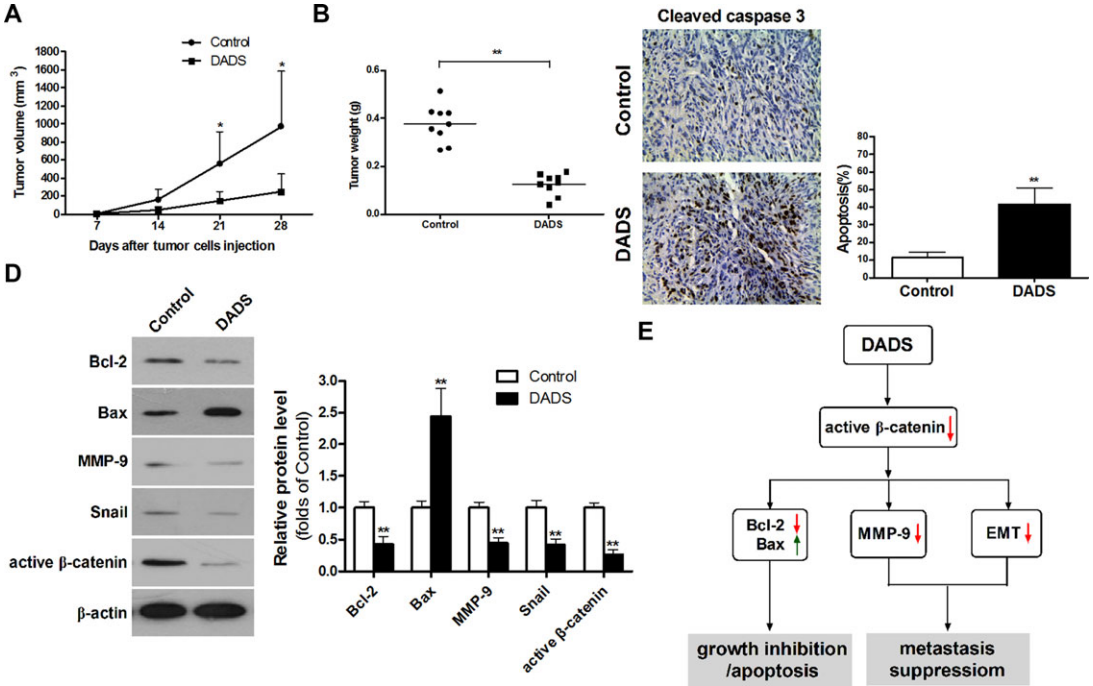

Figure 8. The antitumor activity of DADS in an MDA-MB-231 breast cancer model. (A and B) The volume and weight of tumors from different groups were measured. The mice were injected subcutaneously with MDA-MB-231 cells (2×10^6) on the right rear flank, and were then injected intraperitoneally (i.p.) once every 4 days with 100 μl of vehicle only (PBS) or DADS (100 mg/kg weight). The tumor diameters were measured every week. After 4 weeks of treatment, the mice were euthanized via CO_2 asphyxiation. The tumors were then removed and weighed. (C) Apoptosis was detected by immunohistochemistry staining for cleaved caspase 3 (original magnification: 400×). The stained and unstained cells were counted to determine the percentage of positive cells in each group. (D) The expression of Bcl-2, Bax, MMP-9, Snail, and active β-catenin in the tumor tissues was measured by Western blot. β-actin was used as an internal loading control. The data are presented as the mean ± SD ($n = 9$). *$p < 0.05$ and **$p < 0.01$ (versus control group). (E) Proposed mechanism showing DADS-mediated cell growth inhibition and metastasis suppression in TNBC cells.

increase in apoptosis (cleaved caspase 3 staining) in tumors from DADS-treated mice (Fig. 8C). Furthermore, Western blot analysis revealed decreased expression of Bcl-2, MMP-9, Snail, and active β-catenin, and increased expression of Bax in mice treated with DADS (Fig. 8D). These results correlate well with our in vitro results, demonstrating that DADS markedly inhibits breast cancer development.

4 Discussion

Several studies have suggested that DADS might induce caspase-dependent apoptosis in various cancer cell types through a mitochondria-mediated intrinsic pathway. DADS induced apoptosis in B16F-10 melanoma cells by activating caspase-3 and downregulating Bcl-2 expression [24]. Bcl-2 expression was also significantly decreased in DADS-treated human prostate cancer PC-3 cells and lung adenocarcinoma A549 cells [25, 26]. In addition, DADS induced caspase-dependent apoptosis in human cancer cells through a Bax-triggered mitochondrial pathway [27]. Inhibition of caspase-3 activation completely blockaded DADS-induced apoptosis in mouse-rat hybrid retina ganglion N18 cells and human colon cancer COLO 205 cells [28, 29]. Studies regarding the proapoptotic effect of DADS in breast cancer cells have been performed primarily in the human breast cancer cell line MCF-7 (ER+/PR+/HER2-). In addition to induction of the Bax-triggered mitochondrial pathway, inhibition of ERK and histone deacetylation and activation of the JNK and p38 pathways have also been implicated in DADS-induced apoptosis in MCF-7 cells [30–32]. In this study, we confirmed the proapoptotic activity of DADS in TNBC cell lines and a mouse xenograft tumor model, and observed that DADS regulated Bcl-2 and Bax expression in a dose-dependent manner, which further suggests that Bcl-2 family members are closely involved in DADS-induced apoptosis.

Previous studies have shown that DADS suppressed metastasis in human prostate carcinoma and gastric adenocarcinoma [33, 34]. Similarly, we show that DADS inhibits the metastasis of breast cancer cell lines. MMP/TIMP is a potential therapeutic target for cancer, as increasing evidence has implicated MMP/TIMP in tumor invasion and metastasis [21, 35]. MMP-9, which is an important member of the MMP family, strongly promotes cancer development. MMP-9 is overexpressed in breast cancer and is an effective indicator for breast cancer prognosis [36, 37]. DADS

significantly inhibited cell invasion by reducing MMP-2 and MMP-9 activities in human prostate carcinoma and gastric adenocarcinoma [33, 34]. In this study, we show that decreased MMP-9 expression and activity may contribute to the antimetastatic effect of DADS treatment in TNBC cells.

In addition to MMP/TIMP, EMT is also closely linked to cancer metastasis. Furthermore, EMT could result in cancer stem cell transformation, drug resistance, immunosuppression, and poorer prognosis for various types of human cancer. Therefore, pharmacologic inhibition of EMT or induction of mesenchymal–epithelial transition (MET) could be instrumental for cancer prevention and treatment [38–40]. Another garlic extract, S-allylcysteine, has been reported to reverse EMT in human oral cancer [41]. In this study, we demonstrated that treatment with DADS reversed EMT in two breast cancer cell lines. These data strongly suggest that DADS could be applied as a potential chemopreventative and chemotherapeutic agent.

β-catenin, a key component of the Wnt/β-catenin signaling pathway, interacts with the TCF/LEF family of transcription factors to activate the transcription of downstream target genes. The β-catenin pathway is closely related to breast cancer cell survival, proliferation, migration, and angiogenesis [42–45]. The β-catenin pathway regulates Bcl-2 activity in colon tumor progression and ischemic preconditioning-mediated cardioprotection [46, 47]. Furthermore, β-catenin promotes the survival of renal epithelial cells by inhibiting Bax [48]. In this study, we show that treatment with DADS significantly decreases Bcl-2 expression and increases Bax expression in TNBC cells by inhibiting the β-catenin signaling pathway. These data suggest that inhibition of the β-catenin pathway induced cancer cell apoptosis by modulating the expression of Bcl-2 family members. It has been reported that aberrant β-catenin signaling is associated with increased MMP expression, and that some MMP family members such as MMP-1, MMP-7, and MMP-9 are downstream targets of the β-catenin pathway [49–51]. Moreover, a number of studies have shown that the β-catenin pathway plays a critical role in promoting EMT, while inhibiting this pathway can reverse the EMT [52–54]. In this study, we show that treatment with DADS reduces metastasis by inhibiting β-catenin and therefore modulating MMP-9 expression and EMT.

Taken together, our results strongly suggest that DADS induces apoptosis and inhibits metastasis in breast cancer cells through modulation of the β-catenin signaling pathway (Fig. 8E). We propose that DADS could be an effective supplement to traditional chemotherapies for breast cancer patients, and that further investigation and clinical trials are warranted.

This study was supported by National Natural Science Foundation of China (81472475 and 81102007), International S&T Cooperation Program of China (ISTCP) (2012DFA10650), and National High Technology Research and Development Program of China (863 Program) (2012AA020101).

The authors have declared no conflict of interest.

5 References

[1] DeSantis, C., Siegel, R., Bandi, P., Jemal, A., Breast cancer statistics, 2011. *CA Cancer J. Clin.* 2011, *61*, 409–418.

[2] Jemal, A., Bray, F., Center, M. M., Ferlay, J. et al., Global cancer statistics. *CA Cancer J. Clin.* 2011, *61*, 69–90.

[3] Reddy, K. B., Triple-negative breast cancers: an updated review on treatment options. *Curr. Oncol.* 2011, *18*, e173–e179.

[4] Saquib, J., Rock, C. L., Natarajan, L., Saquib, N. et al., Dietary intake, supplement use, and survival among women diagnosed with early-stage breast cancer. *Nutr. Cancer* 2011, *63*, 327–333.

[5] Jiang, J., Wojnowski, R., Jedinak, A., Sliva, D., Suppression of proliferation and invasive behavior of human metastatic breast cancer cells by dietary supplement BreastDefend. *Integr. Cancer Ther.* 2011, *10*, 192–200.

[6] Park, H. Y., Kim, N. D., Kim, G. Y., Hwang, H. J. et al., Inhibitory effects of diallyl disulfide on the production of inflammatory mediators and cytokines in lipopolysaccharide-activated BV2 microglia. *Toxicol. Appl. Pharmacol.* 2012, *262*, 177–184.

[7] Busquet, M., Calsamiglia, S., Ferret, A., Carro, M. D. et al., Effect of garlic oil and four of its compounds on rumen microbial fermentation. *J. Dairy Sci.* 2005, *88*, 4393–4404.

[8] Yi, L., Su, Q., Molecular mechanisms for the anti-cancer effects of diallyl disulfide. *Food Chem. Toxicol.* 2013, *57*, 362–370.

[9] Tang, H., Kong, Y., Guo, J., Tang, Y. et al., Diallyl disulfide suppresses proliferation and induces apoptosis in human gastric cancer through Wnt-1 signaling pathway by up-regulation of miR-200b and miR-22. *Cancer Lett.* 2013, *340*, 72–81.

[10] Wen, J., Zhang, Y., Chen, X., Shen, L. et al., Enhancement of diallyl disulfide-induced apoptosis by inhibitors of MAPKs in human HepG2 hepatoma cells. *Biochem. Pharmacol.* 2004, *68*, 323–331.

[11] Shin, D. Y., Kim, G. Y., Lee, J. H., Choi, B. T. et al., Apoptosis induction of human prostate carcinoma DU145 cells by diallyl disulfide via modulation of JNK and PI3K/AKT signaling pathways. *Int. J. Mol. Sci.* 2012, *13*, 14158–14171.

[12] Hui, C., Jun, W., Ya, L. N., Ming, X., Effect of Allium sativum (garlic) diallyl disulfide (DADS) on human non-small cell lung carcinoma H1299 cells. *Trop. Biomed.* 2008, *25*, 37–45.

[13] Teyssier, C., Guenot, L., Suschetet, M., Siess, M. H., Metabolism of diallyl disulfide by human liver microsomal cytochromes P-450 and flavin-containing monooxygenases. *Drug Metab. Dispos.* 1999, *27*, 835–841.

[14] Cole, L., Anderson, M., Antin, P. B., Limesand, S. W., One process for pancreatic beta-cell coalescence into islets involves an epithelial-mesenchymal transition. *J. Endocrinol.* 2009, *203*, 19–31.

[15] Luo, J., Deng, Z. L., Luo, X., Tang, N. et al., A protocol for rapid generation of recombinant adenoviruses using the AdEasy system. *Nat. Protoc.* 2007, *2*, 1236–1247.

[16] Li, H., Huang, J., Yang, B., Xiang, T. et al., Mangiferin exerts antitumor activity in breast cancer cells by regulating

matrix metalloproteinases, epithelial to mesenchymal transition, and beta-catenin signaling pathway. *Toxicol. Appl. Pharmacol*. 2013, *272*, 180–190.

[17] Yang, J. S., Kok, L. F., Lin, Y. H., Kuo, T. C. et al., Diallyl disulfide inhibits WEHI-3 leukemia cells in vivo. *Anticancer Res*. 2006, *26*, 219–225.

[18] Olsson, M., Zhivotovsky, B., Caspases and cancer. *Cell Death Differ*. 2011, *18*, 1441–1449.

[19] Yip, K. W., Reed, J. C., Bcl-2 family proteins and cancer. *Oncogene*. 2008, *27*, 6398–6406.

[20] Liedtke, C., Mazouni, C., Hess, K. R., Andre, F. et al., Response to neoadjuvant therapy and long-term survival in patients with triple-negative breast cancer. *J. Clin. Oncol*. 2008, *26*, 1275–1281.

[21] Rydlova, M., Holubec, L., Jr., Ludvikova, M., Jr., Kalfert, D. et al., Biological activity and clinical implications of the matrix metalloproteinases. *Anticancer Res*. 2008, *28*, 1389–1397.

[22] Gomes, L. R., Terra, L. F., Sogayar, M. C., Labriola, L., Epithelial-mesenchymal transition: implications in cancer progression and metastasis. *Curr. Pharm. Biotechnol*. 2011, *12*, 1881–1890.

[23] Clevers, H., Nusse, R., Wnt/beta-catenin signaling and disease. *Cell*. 2012, *149*, 1192–1205.

[24] Pratheeshkumar, P., Thejass, P., Kutan, G., Diallyl disulfide induces caspase-dependent apoptosis via mitochondria-mediated intrinsic pathway in B16F-10 melanoma cells by up-regulating p53, caspase-3 and down-regulating pro-inflammatory cytokines and nuclear factor-kappabeta-mediated Bcl-2 activation. *J. Environ. Pathol. Toxicol. Oncol*. 2010, *29*, 113–125.

[25] Gayathri, R., Gunadharini, D. N., Arunkumar, A., Senthilkumar, K. et al., Effects of diallyl disulfide (DADS) on expression of apoptosis associated proteins in androgen independent human prostate cancer cells (PC-3). *Mol. Cell. Biochem*. 2009, *320*, 197–203.

[26] Wu, X. J., Hu, Y., Lamy, E., Mersch-Sundermann, V., Apoptosis induction in human lung adenocarcinoma cells by oil-soluble allyl sulfides: triggers, pathways, and modulators. *Environ. Mol. Mutagen*. 2009, *50*, 266–275.

[27] Nagaraj, N. S., Anilakumar, K. R., Singh, O. V., Diallyl disulfide causes caspase-dependent apoptosis in human cancer cells through a Bax-triggered mitochondrial pathway. *J. Nutr. Biochem*. 2010, *21*, 405–412.

[28] Lin, H. L., Yang, J. S., Yang, J. H., Fan, S. S. et al., The role of Ca2+ on the DADS-induced apoptosis in mouse-rat hybrid retina ganglion cells (N18). *Neurochem. Res*. 2006, *31*, 383–393.

[29] Yang, J. S., Chen, G. W., Hsia, T. C., Ho, H. C. et al., Diallyl disulfide induces apoptosis in human colon cancer cell line (COLO 205) through the induction of reactive oxygen species, endoplasmic reticulum stress, caspases casade and mitochondrial-dependent pathways. *Food Chem. Toxicol*. 2009, *47*, 171–179.

[30] Altonsy, M. O., Habib, T. N., Andrews, S. C., Diallyl disulfide-induced apoptosis in a breast-cancer cell line (MCF-7) may be caused by inhibition of histone deacetylation. *Nutr. Cancer* 2012, *64*, 1251–1260.

[31] Na, H. K., Kim, E. H., Choi, M. A., Park, J. M. et al., Diallyl trisulfide induces apoptosis in human breast cancer cells through ROS-mediated activation of JNK and AP-1. *Biochem. Pharmacol*. 2012, *84*, 1241–1250.

[32] Lei, X. Y., Yao, S. Q., Zu, X. Y., Huang, Z. X. et al., Apoptosis induced by diallyl disulfide in human breast cancer cell line MCF-7. *Acta Pharmacol. Sin*. 2008, *29*, 1233–1239.

[33] Shin, D. Y., Kim, G. Y., Kim, J. I., Yoon, M. K. et al., Anti-invasive activity of diallyl disulfide through tightening of tight junctions and inhibition of matrix metalloproteinase activities in LNCaP prostate cancer cells. *Toxicol. In Vitro* 2010, *24*, 1569–1576.

[34] Park, H. S., Kim, G. Y., Choi, I. W., Kim, N. D. et al., Inhibition of matrix metalloproteinase activities and tightening of tight junctions by diallyl disulfide in AGS human gastric carcinoma cells. *J. Food Sci*. 2011, *76*, T105–T111.

[35] Roy, R., Yang, J., Moses, M. A., Matrix metalloproteinases as novel biomarkers and potential therapeutic targets in human cancer. *J. Clin. Oncol*. 2009, *27*, 5287–5297.

[36] Scorilas, A., Karameris, A., Arnogiannaki, N., Ardavanis, A. et al., Overexpression of matrix-metalloproteinase-9 in human breast cancer: a potential favourable indicator in node-negative patients. *Br. J. Cancer* 2001, *84*, 1488–1496.

[37] Ranogajec, I., Jakic-Razumovic, J., Puzovic, V., Gabrilovac, J., Prognostic value of matrix metalloproteinase-2 (MMP-2), matrix metalloproteinase-9 (MMP-9) and aminopeptidase N/CD13 in breast cancer patients. *Med. Oncol*. 2012, *29*, 561–569.

[38] Dave, B., Mittal, V., Tan, N. M., Chang, J. C., Epithelial-mesenchymal transition, cancer stem cells and treatment resistance. *Breast Cancer Res*. 2012, *14*, 202.

[39] Foroni, C., Broggini, M., Generali, D., Damia, G., Epithelial-mesenchymal transition and breast cancer: role, molecular mechanisms and clinical impact. *Cancer Treat Rev*. 2012, *38*, 689–697.

[40] Voulgari, A., Pintzas, A., Epithelial-mesenchymal transition in cancer metastasis: mechanisms, markers and strategies to overcome drug resistance in the clinic. *Biochim. Biophys. Acta* 2009, *1796*, 75–90.

[41] Pai, M. H., Kuo, Y. H., Chiang, E. P., Tang, F. Y., S-Allylcysteine inhibits tumour progression and the epithelial-mesenchymal transition in a mouse xenograft model of oral cancer. *Br. J. Nutr*. 2012, *108*, 28–38.

[42] Prosperi, J. R., Goss, K. H., A Wnt-ow of opportunity: targeting the Wnt/beta-catenin pathway in breast cancer. *Curr. Drug Targets*. 2010, *11*, 1074–1088.

[43] Nakopoulou, L., Gakiopoulou-Givalou, H., Karayiannakis, A. J., Giannopoulou, I. et al., Abnormal alpha-catenin expression in invasive breast cancer correlates with poor patient survival. *Histopathology* 2002, *40*, 536–546.

[44] Calaf, G. M., Alvarado, M. E., Hei, T. K., Beta catenin is associated with breast cancer progression in vitro. *Int. J. Oncol*. 2005, *26*, 913–921.

[45] King, T. D., Suto, M. J., Li, Y., The Wnt/beta-catenin signaling pathway: a potential therapeutic target in the treatment of triple negative breast cancer. *J. Cell. Biochem.* 2012, *113*, 13–18.

[46] Li, Q., Dashwood, W. M., Zhong, X., Nakagama, H. et al., Bcl-2 overexpression in PhIP-induced colon tumors: cloning of the rat Bcl-2 promoter and characterization of a pathway involving beta-catenin, c-Myc and E2F1. *Oncogene* 2007, *26*, 6194–6202.

[47] Thirunavukkarasu, M., Han, Z., Zhan, L., Penumathsa, S. V. et al., Adeno-sh-beta-catenin abolishes ischemic preconditioning-mediated cardioprotection by downregulation of its target genes VEGF, Bcl-2, and survivin in ischemic rat myocardium. *Antioxid. Redox Signal*. 2008, *10*, 1475–1484.

[48] Wang, Z., Havasi, A., Gall, J. M., Mao, H. et al., Beta-catenin promotes survival of renal epithelial cells by inhibiting Bax. *J. Am. Soc. Nephrol*. 2009, *20*, 1919–1928.

[49] Zeng, Q., Li, W., Lu, D., Wu, Z. et al., CD146, an epithelial-mesenchymal transition inducer, is associated with triple-negative breast cancer. *Proc. Natl. Acad. Sci. USA* 2012, *109*, 1127–1132.

[50] Saha, S., Duan, X., Wu, L., Lo, P. K. et al., Electrospun fibrous scaffolds promote breast cancer cell alignment and epithelial-mesenchymal transition. *Langmuir* 2012, *28*, 2028–2034.

[51] Raimondi, C., Gradilone, A., Naso, G., Vincenzi, B. et al., Epithelial-mesenchymal transition and stemness features in circulating tumor cells from breast cancer patients. *Breast Cancer Res. Treat*. 2011, *130*, 449–455.

[52] Blick, T., Hugo, H., Widodo, E., Waltham, M. et al., Epithelial mesenchymal transition traits in human breast cancer cell lines parallel the CD44(hi/)CD24 (lo/-) stem cell phenotype in human breast cancer. *J. Mammary Gland Biol. Neoplasia* 2010, *15*, 235–252.

[53] Pin, A. L., Huot, J., β5 integrin orchestrates epithelial mesenchymal transition in breast cancer: comment on: Bianchi A. et al. Cell Cycle 2010; 9:1647–1659. *Cell Cycle.* 2010, *9*, 1873.

[54] Radisky, E. S., Radisky, D. C., Matrix metalloproteinase-induced epithelial-mesenchymal transition in breast cancer. *J. Mammary Gland Biol. Neoplasia* 2010, *15*, 201–212.

